High power, single-mode operation from photonic-lattice semiconductor lasers with controllable lateral resonance

Shuang Li, Dapeng Xu, and Dan Botez[a)]
Reed Center for Photonics, University of Wisconsin, Madison, Wisconsin 53706

(Received 8 August 2005; accepted 18 January 2006; published online 2 March 2006)

An *active-photonic-crystal* (APC) laser based on laterally resonant arrays of antiguides is proposed and demonstrated. Approximately 1-μm-wide, high-index APC sites are obtained by preferential etching and GaAs regrowth into a GaAs/InGaP/AlGaAs base structure. For 4-μm-wide, low-index APC sites ~0.28-μm-thick regrowths provide resonant leaky-wave coupling across a 100-μm-wide aperture (i.e., across a 20-element APC structure) at 0.98 μm vacuum wavelength. Large intermodal discrimination favoring in-phase mode operation to high drive levels is obtained at and around the in-phase mode resonance by introducing significant nonsaturatable losses in the high-index sites. The lateral-resonance condition is controlled during fabrication via small variations in the preferential-regrowths thickness on several pieces from the same wafer base. Virtually single-lobe, near-diffraction-limited beam operation is obtained up to 1.1 W peak power at 11 times threshold. This also represents the demonstration of the lateral component needed for the realization of two-dimensional (2D) grating surface-emitting, single-mode APC lasers. © *2006 American Institute of Physics*. [DOI: 10.1063/1.2180443]

Resonant antiguided laser arrays [so-called resonant-optical-waveguide (ROW) arrays][1,2] have demonstrated operation in near-diffraction-limited beams to watt-range powers in both pulsed[3] and continuos-wave (CW) regimes.[4] The ROW array was shown more than a decade ago[5] to be analogous to a second-order distributed feedback (DFB) structure in the *lateral* propagation direction, for which the Bragg condition is exactly satisfied and the modes are band-edge solutions. Periodic gain modulation selects operation in a large, single spatial mode. Thus the ROW array was *the first* active-photonic-crystal (APC) structure for (lateral) spatial-mode selection and control in large-aperture ($\geqslant$100 μm) semiconductor diode lasers. The analogy to DFB structures was further extended[6] by deriving the equations for the lateral-wave amplitudes, which are found to be identical to the well-known coupled-wave equations in DFB-laser theory[7] since, at and near the resonance condition, the reflectance of a lateral wave from one cell of the APC structure is quite small.[6,8] Unlike the vast majority of one-dimensional (1D) APC devices, for ROW arrays the gain is preferentially enhanced on the *low-index* crystal sites,[1,2,9] which in turn favors lasing of only the leaky-wave modes of the periodic structure.

Conventional ROW arrays have *p*-cladding layer thicknesses of typical values: 1–1.5 μm. High-(effective)-index interelement regions are formed by burying *n*-GaAs islands deep inside the *p*-cladding layers, in close proximity to the active region. Thus one cannot insure during the device fabrication that the lateral resonance condition will be fulfilled.

Here we present a different type of ROW-array structure. Compared to conventional devices, it has a thinner *p*-cladding layer (only 0.4 μm compared to 1.5 μm) and the high-index GaAs islands are formed by regrowth into the device top part, such that they end up in contact with the *p*-side metallization. This device has two main advantages: (1) Strong intermodal discrimination can be provided via nonsaturable absorption losses to the *p*-metal and/or free-carrier absorption in the region material; (2) the lateral resonance can be readily achieved by varying the regrown-material thickness during fabrication. This also represents the first experimental demonstration of the lateral component of a recently proposed 2D APC structure[9,10] for the generation of watt-range, single-mode surface-emitted power. (The longitudinal component of the 2D APC surface-emitting devices: second-order DFB grating with a central π phase shift, has already been demonstrated.[11])

A cross-sectional view of the APC laser structure is shown in Fig. 1. Initially we grow a base structure designed for lasing at 0.98 μm. The base structure has a 1-μm-thick *n*-$Al_{0.54}Ga_{0.46}As$ lower cladding layer. Optical confinement and gain are provided by a SCH-DQW structure consisting of 0.1-μm-thick $Al_{0.4}Ga_{0.6}As$ optical-confinement layers surrounding two 70-Å-thick $In_{0.2}Ga_{0.8}As$ quantum wells. The 0.4 μm *p*-cladding layer is formed of *p*-$Al_{0.54}Ga_{0.46}As$ (0.2 μm) and *p*-InGaP (0.2 μm), both doped at 5×10^{17} cm^{-3}. The base is then capped with a 0.1-μm-thick p^+-GaAs layer doped at 3×10^{19} cm^{-3}. Then, by using a SiO_2 mask, ~1-μm-wide and 0.28-μm-thick *p*-GaAs regions are formed by preferential etch and regrowth. The regrown *p*-GaAs regions provide the high-effective-index sites of the APC structure (see the effective-index profile at the top of Fig. 1). When the element region are 4-μm-wide and the interelement spacing, *s*, is ~1.0 μm, 0.28-μm-thick *p*-GaAs regrown regions assure the necessary lateral-resonance condition (determined by using rigorous 2D modeling[12]) as well as a large (lateral) effective-index step ($\Delta n_{eff}\sim0.055$).

As shown in Fig. 1, the transverse fields in the high-index APC sites are "drawn" into the high-index, regrown *p*-GaAs regions, thus experiencing strong losses to the *p*-metal (i.e., Au), whereas the fields in the low-index sites have negligible overlap with the *p*-metal. Just as for conventional ROW arrays, the modal gain is strongly enhanced in the low-index sites, which in turn favors oscillation of only the leaky modes of the APC structure (i.e., the modes whose

[a)]Electronic mail: botez@engr.wisc.edu

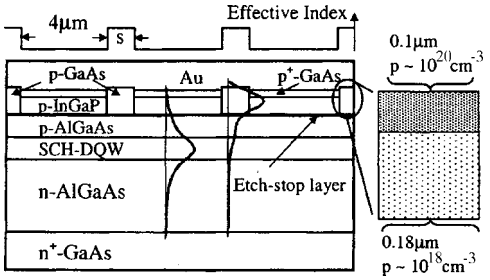

FIG. 1. Schematic device cross section with transverse-field profiles in the low- and high-index sites of the APC structure. Details of the preferentially regrown GaAs region are shown in the blown-up portion.

main intensity peaks reside in the low-index sites). We plot in Fig. 2 the percentage of the field intensity in the *low-index* sites, so-called elemental confinement factor, Γ_{el}, for relevant modes of a 20-element structure as a function of the thickness of the regrown *p*-GaAs material, *t*. The curves are shown around the *t* value of 0.28 μm, which corresponds to the lateral resonance of the desired (in-phase) mode for a 20-element device (i.e., mode 38).[12] Modes 37 and 39 are the lower and upper adjacent modes, respectively, while 19 and 57 are out-of-phase modes.[12] As expected[13] at and near its resonance mode 38 has most of its energy; ~99%, in the low-index sites. In contrast the competing modes have Γ_{el} values $\leqslant$85%, and thus are subject to strong absorption losses in the high-index sites.

To assess the overall intermodal discrimination we calculated the threshold-current density, J_{th}, for the same modes as in Fig. 2 around the in-phase mode resonance (i.e., t_{res} =0.28 μm). The cavity length is taken to be 700 μm and the facets are uncoated. Figure 3(a) shows the case when the loss in the high-index sites is primarily due to absorption in the metal (i.e., Au). The-in-phase mode (i.e., mode 38) is found to be favored to lase at and near its resonance, but the discrimination is rather weak, since the competing modes have J_{th} values only about 5% higher than the in-phase mode.

Further intermodal discrimination is obtained by introducing strong free-carrier absorption in the high-index sites. We achieved that by heavily doping (10^{20} cm^{-3}) with carbon only the top part of the regrown *p*-GaAs region, as shown in Fig. 1 (the free-carrier absorption coefficient, α_{fc}, in the carbon-doped GaAs is ~600 cm^{-1}). This is nonsaturatable loss, since carriers absorbed in the p^+-GaAs layers are swept away to the metal contact, and thus one can prevent self-pulsations due to saturable absorption.[14] As seen from Fig. 3(b), at resonance, the in-phase mode is hardly affected; only a 2% increase in J_{th}; while the J_{th} values for the competing modes increase by ~30% compared to the case of no heavily-doped regrowths [Fig. 3(a)]. Now the J_{th} of the competing modes, compared to the J_{th} of the in-phase mode, is ~15% larger over a 0.02-μm-wide range in *t*, and more than 20% larger over a 0.01 μm range in *t*. Since the in-phase mode has a uniform intensity profile at and near its resonance[2] multimoding due to gain spatial hole burning at high drives above threshold is not an issue.[15] Furthermore, the strong intermodal discrimination is achieved without the need for intracavity Talbot-type spatial filters,[2–4] which can cause self-pulsations.[16]

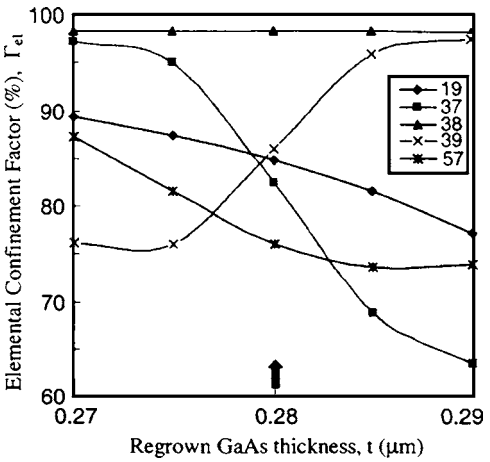

FIG. 2. Percentage of the field intensity residing in the low-index APC sites for modes of a 20-element structure as a function of the thickness of the regrown *p*-GaAs material. Mode 38 is the in-phase mode (Ref. 12), modes 37 and 39 are adjacent modes, and modes 19 and 57 are out-of-phase modes. The vertical arrow indicates the in-phase mode (lateral) resonance.

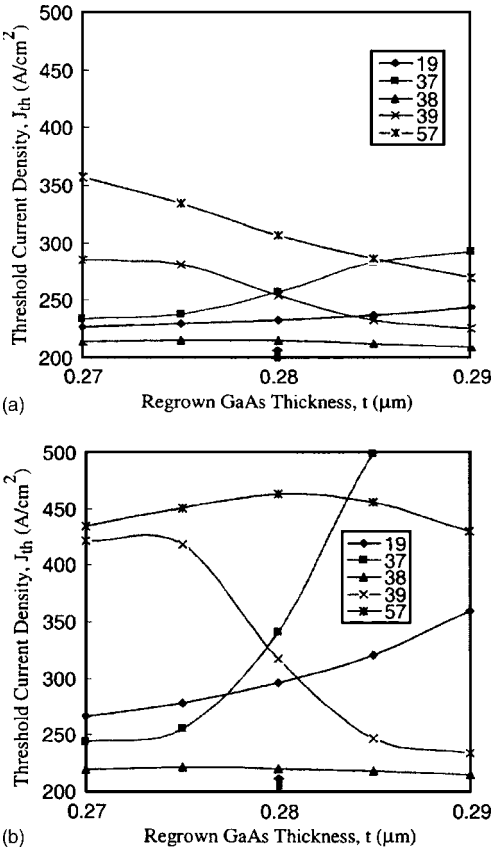

FIG. 3. Threshold-current densities of relevant modes of a 20-element APC structure vs the thickness of the regrown *p*-GaAs material. (a) No free-carrier absorption loss in the high-index sites; (b) free-carrier absorption from the heavily doped portion of the regrown material (Fig. 1).

To insure that a laterally resonant array is readily achieved the following procedure is followed. A 100-nm-thick SiO_2 film is deposited on the grown base structure. The array pattern is then transferred into the SiO_2 film by photolithography and wet etching, thus creating a hard mask for trench etching and preferential regrowth. Nominally 1-μm-wide trenches are formed by wet etching the *p*-GaAs cap (0.1 μm) and *p*-InGaP (0.2 μm) part of the cladding layer (see Fig. 1) over a 2-in.-diameter wafer. Then the actual trench width is measured using a scanning electron microscope (SEM). Calculations are then performed to estimate the regrown material thickness needed for lateral reso-

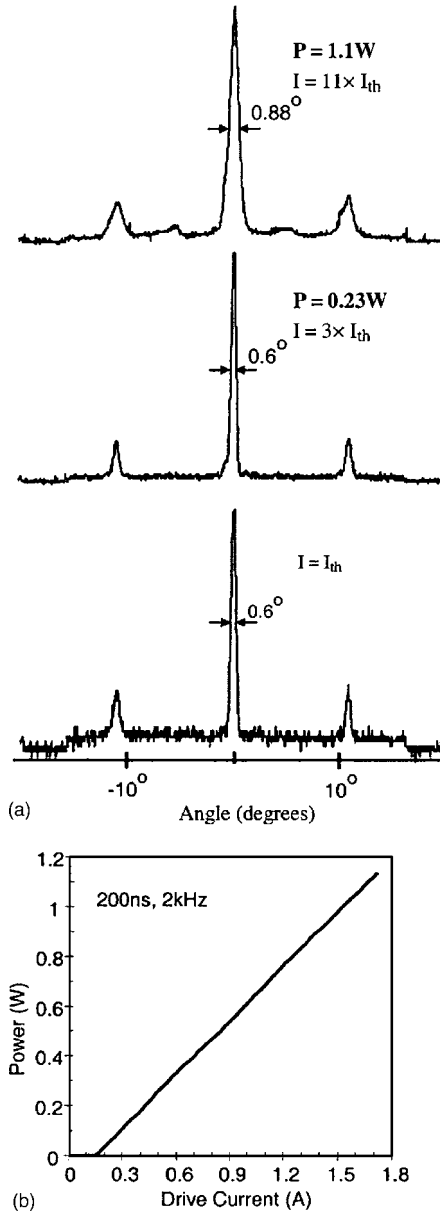

FIG. 4. Characteristics of 20-element device of 100 μm aperture and uncoated facets: (a) Lateral far-field patterns as a function of the drive level above threshold, I_{th}. The diffraction limit is 0.6°. I_{th} is 156 mA. (b) Light-current curve in pulsed operation.

nance, t_{res}. The wafer is broken into three pieces and preferential *p*-GaAs regrowths of slightly different thicknesses: t_{res}, $t_{res}+0.01$ μm, and $t_{res}-0.01$ μm, are performed. After the regrowths the SiO_2 masks are removed and the pieces of wafer are processed. Measurements of the far field patterns of chips from the three wafer pieces determine which wafer piece best meets the lateral resonance condition. Thus by slightly varying the regrowth thickness, and subsequently slightly changing the effective index in the high-index sites, one can "tune" the devices into resonance.

Figure 4 shows preliminary experimental results from 20-element arrays of 100-μm-wide aperture and 700-μm-long cavity with as-cleaved facets. Outside the APC structure the current is confined via SiO_2 and etched grooves. The *p*-metallization consists of unalloyed Au atop the array. We have achieved near-diffraction-limited beam operation [Fig. 4(a)] up to 1.1 W peak pulsed (200 ns, 2 kHz) power at 11× threshold. Optimized, facet-coated (HR/AR) devices are likely to provide even higher coherent powers. At 11× threshold the farfield main lobe's FWHM is only 0.88°, which corresponds to 1.45 times the diffraction limit. Above 1.1 W the beam broadens due to *intraelement* gain spatial hole burning (GSHB),[15] which can be alleviated by narrowing the width of the low-index sites (e.g., from 4 μm to 3 μm). Then the high-index-sites' width needs to be narrowed accordingly (i.e., from 1 μm to 0.75 μm) to maintain the same high percentage of energy in the central lobe.[12] The light-current curve is shown in Fig. 4(b). The slope efficiency is 0.73 W/A, which indicates an internal loss coefficient, α_i, of 9 cm^{-1} for these unoptimized devices. However, α_i values as low as 5 cm^{-1} and CW operation can be obtained from thin-clad, unalloyed-Au-contact devices[17] by using heavily doped, cladding material for the cap layer.

Moreover, this device structure is intended to be used in 2D APC grating surface-emitting structures,[10] which due to the strong built-in index profile ($\Delta n > 0.05$) in the lateral APC component, strong intermodal discrimination, and uniform guided-field distributions in *both* the lateral and longitudinal directions hold the promise for stable single-mode, single-lobe surface-emitted CW power in the 2–3 W range.[10]

In conclusion, we present a new type of APC laser for stable, spatial single-mode operation. Strong intermodal discrimination is provided by nonsaturatable losses from the *p*-metal and free-carrier absorption in the high-index APC sites. The lateral resonance can be readily achieved by varying, during the device fabrication, the thickness of *p*-GaAs material regrown for the formation of the high-index sites. Preliminary results are quite promising: 1.1 W near-diffraction-limited power from 100-μm-wide aperture devices.

This work was supported by NSF Grant No. ECS-0200321.

[1] D. Botez, L. J. Mawst, G. Peterson, and T. J. Roth, Appl. Phys. Lett. **54**, 2183 (1989).
[2] D. Botez, L. J. Mawst, G. L. Peterson, and T. J. Roth, IEEE J. Quantum Electron. **26**, 482 (1990).
[3] H. Yang, L. J. Mawst, M. Nesnidal, J. Lopez, A. Bhattacharya, and D. Botez, Electron. Lett. **33**, 136 (1997).
[4] H. Yang, L. J. Mawst, and D. Botez, Appl. Phys. Lett. **76**, 1219 (2000).
[5] C. Zmudzinski, D. Botez, and L. J. Mawst, Appl. Phys. Lett. **60**, 1049 (1992).
[6] A. P. Napartovich and D. Botez, Proc. SPIE **2994**, 600 (1997).
[7] H. Kogelnik and C. V. Shank, J. Appl. Phys. **43**, 2327 (1972).
[8] D. V. Vysotskii and A. P. Napartovich, J. Exp. Theor. Phys. **88**, 227 (1999).
[9] S. Li, G. Witjaksno, and D. Botez, IEEE Conference Proceedings of the Lasers and Electro-Optics Society, 2003 Annual Meeting, Tucson, AZ, 26–30 October, 2003, Vol. 2, pp. 575–576.
[10] S. Li and D. Botez, IEEE Photon. Technol. Lett. **17**, 519 (2005).
[11] G. Witjaksono, S. Li, J. J. Lee, D. Botez, and W. K. Chan, Appl. Phys. Lett. **83**, 5365 (2003).
[12] D. Botez, *Diode Laser Arrays*, edited by D. Botez and D. R. Scifres (Cambridge University Press, Cambridge, 1994), pp. 1–71.
[13] D. Botez and L. J. Mawst, Appl. Phys. Lett. **60**, 3096 (1992).
[14] S. Ramanujan, H. G. Winful, M. Felisky, R. K. DeFreez, D. Botez, M. Jansen, and P. Wisseman, Appl. Phys. Lett. **64**, 827 (1994).
[15] R. F. Nabiev and D. Botez, IEEE J. Sel. Top. Quantum Electron. **1**, 138 (1995).
[16] R. F. Nabiev, M. D. Iturbe-Castillo, J. J. Sanchez-Mondragon, A. I. Onishchenko, and D. Botez, Appl. Opt. **32**, 4480 (1993).
[17] S. H. Macomber, J. S. Mott, B. D. Schwartz, R. S. Setzko, J. J. Powers, and J. E. Logue, *Conference Proceedings of the IEEE LEOS'96 Annual Meeting* (1996), Vol. 1, p. 11; Proc. SPIE **3001**, 42 (1997).